

NUMERICAL STUDY OF THE STRUCTURE OF THERMAL PLUME IN A VERTICAL CHANNEL: EFFECT OF THE HEIGHT OF CANAL

by

Belgacem JOUINI*, **Mourad BOUTERRA**,
Afif EL CAFSI, and **Ali BELGHITH**

Laboratory for Energy and Heat and Mass Transfer (LETTM),
Faculty of Sciences of Tunis, University of Tunis El Manar, Tunisia

Original scientific paper
DOI: 10.2298/TSCI130123058J

In this paper we present numerical study, using software named Calculation FDS, of thermal plume that evolve from the source at the entrance of a vertical channel. In the literature, there are researchers who are interested in the interaction of plume with confined medium. These studies are based on the determination of the global structure of plume confined. It is found that this plume consists of three distinct zones. First zone near source (instability zone), followed by a second zone, the plume development, and third zone which is the zone of turbulence. Comparing the overall structure of the plume confined to that of the free plume, one can identify the presence of a third zone (zone of instability). The aim is firstly to determine the height of the instability zone located above of source, and secondly, to make a spectral study frequencies exhaust. Thus, effects of geometrical parameters on frequencies of these escapements and height an instability zone can be shown. The final aim is to establish correlations between the dimensionless Strouhal and Grashof numbers.

Key words: numerical study, commercial software computational fluid dynamics, plume thermal, hot springs, vertical channel

Introduction

The thermal plume is a very common phenomenon in our surroundings. This phenomenon can be found in fire, the plant discharges, the chimneys outlet, *etc.* There are numerous investigations on the thermal plume in its free state, without any interaction with the plume. The phenomenon of thermal plume can be accompanied by an interaction with its environment. The thermal plume affects the confinement effect of his environment. Because of interaction of the plume with the thermosiphon, induced flow of the plume confinement, the overall structure is changed by comparison with one of the free plume.

Tan [1] proposes a study of a configuration, aiming to collect solar energy in a sensor facing south and north transfer sensor. The objective of this work is not for direct heating of the interior but to reduce heat loss to the outside. Bezian and Arnaud [2] have developed a system close enough to the firestop wall unlike loan they have disposed of sections filled with water inside the wall sensor. Mohamed *et al.* [3], Bouslimi and Dehmani [4], and Zinoubi *et al.* [5], studied the thermosiphon effect of a thermal plume and a configuration that admits an axial symmetry. They showed that the flow resulting from this interaction has three distinct

* Corresponding author; e-mail: belgacem_jouini@yahoo.fr

areas, as it is an area of instability near the source followed by a development zone and ending with an area of establishment of the turbulence.

Ben Maad [6] studied experimentally and numerically the effect of a heated grid, placed at the entrance of a vertical channel. He is interested in its influence on the flow structure. He found a thermal instability and dynamic fields at the entrance of the channel and an intensification of the coefficient transfer means. Gammoudi *et al.* [7] have worked on improving the efficiency of solar energy passive capture by simulating the problem in the laboratory by the study of a thermal plume generated by a heat source placed in the rectangular input of a vertical channel with heated walls. It was shown that the increase in the source temperature is used to improve the air flow within the system. Naffouti *et al.* [8] investigated experimentally the fine structure of a flow which results from the interaction of a thermal plume with a thermosiphon in a vertical channel. They showed that this flow is composed of three similar distinct zones. Jouini *et al.* [9] conducted a numerical study on the effect of the position of a source of a thermal plume ($T_s = 300\text{ }^\circ\text{C}$) with respect to the input of a vertical channel. This study is based on the finite volume method, using the $k-\varepsilon$ standard model. They found that the size of the recirculation zone depends on the source vertical position with respect to the input channel. This allowed them to prove that the size of this area increases with h (source-channel spacing).

In this work, we made a 2-D numerical study, using fire dynamic simulation calculation software (FDS), a thermal plume placed at the entrance of a vertical channel. In the first part, we did a study on the comparison of numerical results with the results found by Naffouti, *et al.* [8] based on experience. In the second part, we determined the frequency of vortex exhaust rollers formed above the source. Thus, the effect of the shape rate by searching a between correlation Grashof and Strouhal numbers.

Geometric configuration and numerical modeling

Geometric configuration

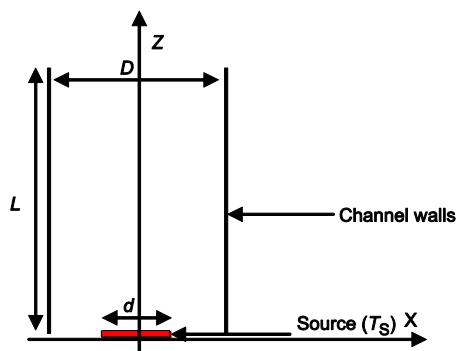


Figure 1. Geometric configuration

In our work we will use the following quantities (fig. 1):

- the width of the heat source $d = 6\text{ cm}$ and this source is placed horizontally at the channel inlet to generate a plume,
- two plates $D = 15\text{ cm}$ apart and length L form the channel, the inner walls of the channel plates are heated uniformly at a temperature of $20\text{ }^\circ\text{C}$,
- the source-channel spacing $h = 0$, and
- the inlet and outlet of the channel are carried out at atmospheric pressure and ambient temperature $T_a = 20\text{ }^\circ\text{C}$ (initially).

Commercial software FDS is used to solve Navier-Stokes equations using large eddy simulation method (LES). This method is based on the averaged equations in the time after the application of the Reynolds decomposition.

Mathematical model

The FDS is being developed at NIST to study fire behavior and to evaluate the performance of fire protection systems in buildings.

The computer program can be used for fire related problems analysis, such as temperature, velocity and concentration distribution, FDS has been formerly successfully applied to study the dispersion of propane under a leakage condition in a room [10], contamination levels in near and far field in a warehouse facility under forced ventilation [11], and was validated [12] to be capable of simulating the transportation of CO species in a channel fire.

FDS solves numerically a form of the Navier-Stokes equations appropriate for low speed, thermally-driven flow with an emphasis on smoke and heat transport from fires. The core algorithm is an explicit predictor-corrector scheme, second order accurate in space and time. Turbulence is treated by the Smagorinsky form of large eddy simulation (LES). It is possible to perform a direct numerical simulation (DNS).

The conservation equations for mass, momentum and energy for a Newtonian fluid are presented here [13].

- Conservation of mass:

$$\frac{\partial \rho}{\partial t} + \nabla(\rho u) = 0$$

- Conservation of momentum:

$$\left(\frac{\partial}{\partial t} \rho u \right) + \nabla \rho u u + \nabla p = \rho g + f_b + \nabla \tau$$

- Transport of sensible enthalpy:

$$\frac{\partial(\rho h_s)}{\partial t} + \nabla \rho h_s u - \frac{Dp}{Dt} = q'' + q_b'' - \nabla q'' + \varepsilon$$

- Equation of state for a perfect gas:

$$p = \frac{\rho R T}{\bar{W}}$$

Turbulence methods commonly used in CFD are based on the Reynolds averaging Navies-Stokes equation (RANS) method, large eddy simulation (LES) and direct numerical simulation (DNS).

In this study large eddy simulation method (LES) is used. The application of LES techniques to fire is aimed at extracting greater temporal and spatial fidelity from fire simulation. The model explicitly calculates the turbulent large scales and models the effects of smaller ones using sub-grid closure rules. For the reacting flows, LES can resolve the instantaneous position of a large-scale flame, so that LES captures the low-frequency variations of flow parameters. The approach based on LES has a particular advantage over the Reynolds-averaging procedures in that only the effects of small-scale turbulence motion have to be modeled. The FDS code adopts the low Mach number combustion equations describing the low speed motion of a gas driven by chemical heat release and buoyancy forces. The balance equations for LES are obtained by filtering the instantaneous balance equations.

In predicting smoke movement by LES, two points should be considered [13, 14]: fine enough grids, and a suitable sub-grid model (SGM) on small eddies.

The LES sub-grid model commonly used in LS was developed originally by Smagorinsky. In LES, the eddy viscosity was obtained by assuming that the small scales are

in equilibrium, by balancing the energy production and dissipation [15, 16]. A refined filtered dynamics sub-grid model was applied in the FDS model to account for the sub-grid scale motion of viscosity, thermal conductivity and material diffusivity [13]. The dynamic viscosity defined in FDS is:

$$\mu_{LES} = \rho (C_s \Delta)^2 \left[2 \overline{S_{ij} S_{ij}} - \frac{2}{3} (\nabla \bar{u})^2 \right]^{1/2}$$

where C_s is the empirical Smagorinsky constant, $\Delta = (\delta x \delta y \delta z)^{1/3}$ and:

$$|S| = 2 \left(\frac{\partial u}{\partial x} \right)^2 + 2 \left(\frac{\partial v}{\partial y} \right)^2 + 2 \left(\frac{\partial w}{\partial z} \right)^2 + \left(\frac{\partial u}{\partial x} + \frac{\partial v}{\partial y} \right)^2 + \left(\frac{\partial u}{\partial z} + \frac{\partial w}{\partial x} \right)^2 + \left(\frac{\partial v}{\partial z} + \frac{\partial w}{\partial y} \right)^2 - \frac{2}{3} (\nabla \cdot \vec{u})^2$$

The term $|S|$ consists of second-order spatial differences averaged at the grid centre. The thermal conductivity k_{LES} and material diffusivity D_{LES} of the fluid are related to the viscosity μ_{LES} in terms of the Prandtl and Schmidt numbers by:

$$k_{LES} = \frac{C_p \mu_{LES}}{Pr}, \quad (\rho D)_{l,LES} = \frac{\mu_{LES}}{Sc}$$

Both Prandtl and Schmidt numbers are assumed to be constant. The specific heat c_p is taken to be that of the dominant species of the mixture. The constants C_s , Pr and Sc are defaulted in FDS as 0.2, 0.5, and 0.5, respectively.

The Courant-Friedrichs-Lewy (CFL) was used in FDS to justify convergence. This criterion is more important for large-scale calculations where convective transport dominates the diffusive one. The estimated velocities are tested at each time step to ensure that the CFL condition is satisfied:

$$\max \left(\frac{|u_{ijk}|}{\delta x}, \frac{|v_{ijk}|}{\delta y}, \frac{|w_{ijk}|}{\delta z} \right) < 1$$

The initial time step was set automatically in FDS by the size of a grid cell divided by flow characteristic velocity. Default values of the initial time step is $5(\delta x \delta y \delta z)^{1/3} / (gH)^{-1/2}$ where δx , δy , and δz are the dimensions of the smallest grid cell, H is the height of the computational domain, and g – the gravitational acceleration [13].

Results and discussion

Comparison of the numerical simulation with experiment

In this part we studied the flow of a thermal plume, from a 6 cm rectangular source and heated to a temperature $T = 300$ °C, within a vertical channel with width of $D = 15$ cm and length of $L = 42$ cm.

Figure 2 represents the temperature and velocity isovalues. It is obvious that there is a formation of flapping over the heat source. These beats have eddies that escape after a well-defined height from the level of the source in the first zone, the air, which is heated after

contact with the surface of the source, riding in the channel as result of the Archimedes force applied to the heated air. The ascendancy of the air in the channel is accompanied by the formation of a large vortex over source. This whirlwind ends up being dropped in the central part of the channel. This phenomenon is an alternative way to either side of the edges of the hot source. The first region is a region of instability. In the central part of the channel, there is smaller tourbillion which characterizes the development area of the plume. Before leaving the channel, the flow becomes more homogeneous.

Figure 3 shows channel feeding through the fresh air at its lower part. From this visualization, the three separate areas of the well that form plume flow confined within the channel. Upward in the channel, the flow becomes more homogeneous.

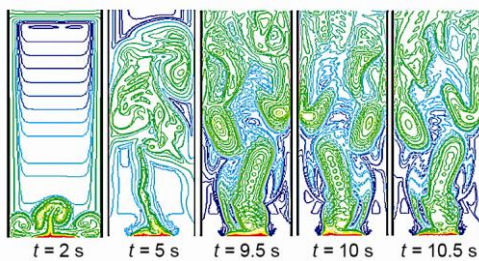


Figure 2. Temperature isovalues for different instants

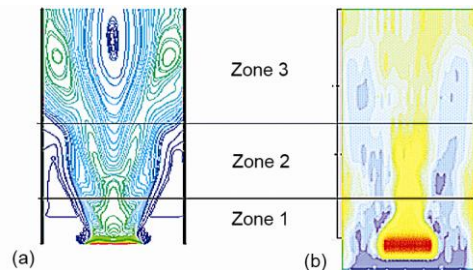


Figure 3. Visualization: (a) numerical, (b) experiment, Naffouti *et al.* [9]

Figures 4 and 5 show the average temperature profiles and average velocity ($Z^* = 0.2$ and 0.92), respectively.

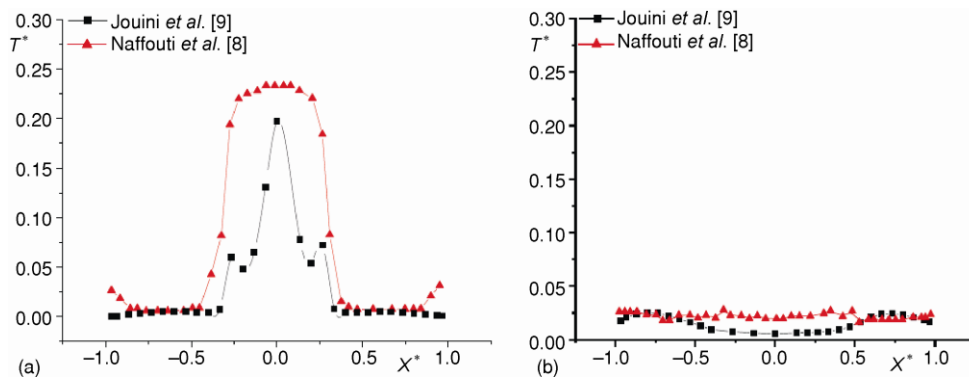


Figure 4. The average temperature profiles for (a) $Z^* = 0.2$, (b) $Z^* = 0.92$

In the lower part of the channel ($Z^* = 0.2$), the temperature profile shows that there are 3 maxima, two at the edges of the source, are symmetrical to the median plane, and the other which is more inclined to the large median. There are also two minimum symmetrical to this plane. The two minimums translating fresh air flow to the heat source side at the ends of the source, hence forming vortices in the lower part of the channel. The velocity profile for the same level admits two peaks symmetrical to the median plane of the channel. These two maxima are results of the supply of the plume by air on both sides of the channel.

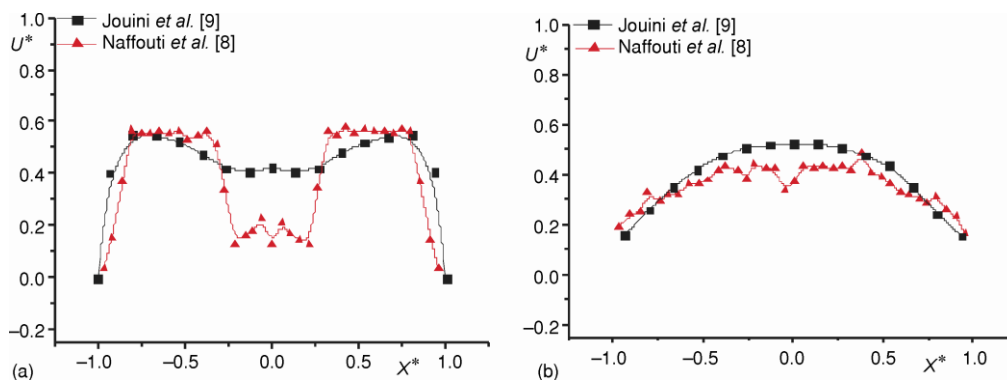


Figure 5. The average velocity profiles for (a) $Z^* = 0.2$, (b) $Z^* = 0.92$

In the upper part of the channel ($Z^* = 0.92$), the profiles of the temperature and speed become flattened. In this level, temperature and speed will be more homogeneous.

The visualization and the profiles of the velocity and temperature show good agreement in the area of development of the plume with experiments, Naffouti *et al.* [8], and the numerical simulation of FDS.

Effect of height channel of the plume on the structure

Thermal and dynamic study

The isovalues of thermal and dynamic fields show that the plume (figs. 6 and 7), which interacts with the inner walls of the channel, is divided into three areas, these areas are shown in many literature sources. The first zone, located adjacent to source, is the region of instability. The second method area, in the central part of the channel, is a plume development area, and the last zone, located in the upper part of the channel, is the zone of turbulence where the plume becomes more homogeneous.

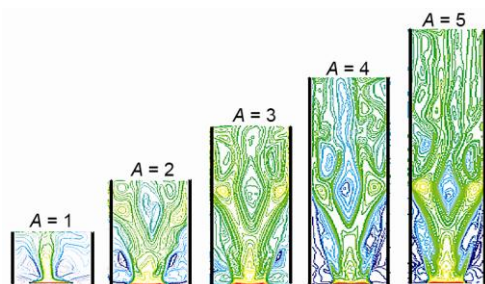


Figure 6. Isovalues of temperature for different shape ratios of channel A instants

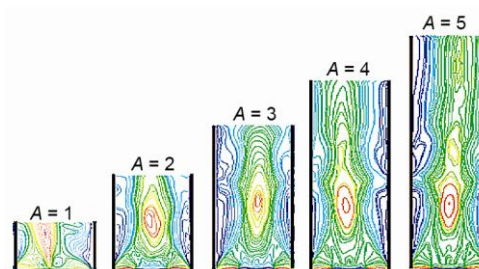


Figure 7. Isovalues of velocity for different shape ratios of channel A

The gradient of the temperature is more important in the first zone, near the source. The gradient decreases with the increase of Z^* . In the central part, vortex structures of small and medium size are currently formed. These vortices are formed after the big exhaust vortex above the source.

It was noted that the dimensionless height of the instability zone (the first zone) is the same regardless of the channel shape ratio. It is clear that the number of small eddies in-

creases with altitude. For better understanding the effect of the channel height, the profiles of the axial average velocity and average temperature were traced (figs. 8 and 9). From figs. 8 and 9 we can conclude that the height of the zone of instability varies linearly with the channel height. This height is located at $Z^* = 0.12$.

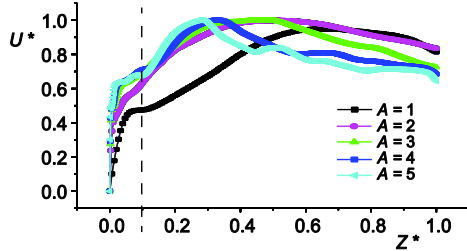


Figure 8. Average velocity profile at the axis of the source

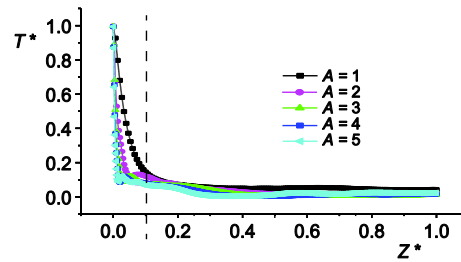


Figure 9. Average temperature profile at the axis of the source

The developing zone of the plume (second zone) is located in the central part of the channel. The axial profile of the average speeds shows that the dimensionless height depends on shape ratio A .

Figure 10 shows that, for shape ratio A less than 2.5, the average velocity at the outlet of the channel increases linearly with the height of the channel. When A has values around 3, the exit velocity remains practically constant. If A exceeds 3.5 this speed continues to increase linearly with the channel height.

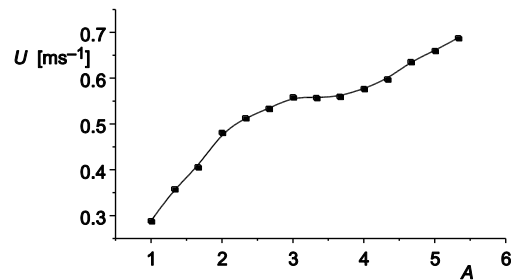


Figure 10. The average velocity profile according to shape ratio

Spectral study

The temporal evolution of the temperature, for different levels in the channel (fig. 11), shows that the beat phenomenon is located in the lower portion of the channel. Hence the fluctuation of the temperature is very important in the first part of the channel (Z^* less than 0.2). For this reason it is taken that the temporal variation of the velocity is in intermediate position of the area beat (instability zone) as $Z^* = 0.12$.

Figures 12 and 13 show the temporal variation of the velocity, for $Z^* = 0.12$ on the axis of the channel, and fluctuation spectrum, respectively. Figure 12 shows the velocity fluctuation over time around an average velocity U . For this reason the study was made based on the effect of shape ratio on the frequency of this fluctuation.

Table 1 shows the escape for each shape ratio A , the average speed, Strouhal and Grashof numbers.

Figure 14 shows that the Strouhal number increases by decreasing the Grashof number. From $A = 2$ ($Gr < 50 \cdot 10^6$), this variation reflects that when the shape ratio A increases (Grashof number decreases), the distance traveled by a fluid particle, in the course of its movement exhaust, increases.

For small values of shape ratio A (large values of Grashof number), the Strouhal number does not admit a well-defined theory (fig. 15).

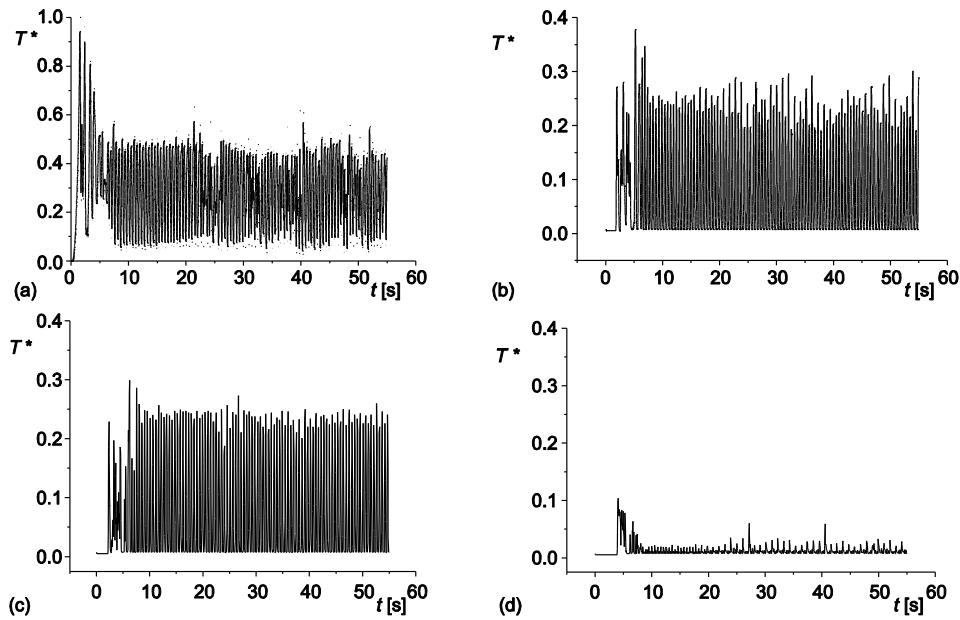


Figure 11. Temporal variation of the temperature; (a) $Z^* = 0.04$, (b) $Z^* = 0.1$, (c) $Z^* = 0.2$, and (d) $Z^* = 0.5$

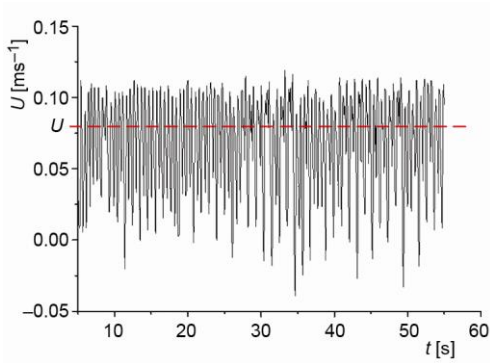


Figure 12. Temporal variation of the velocity

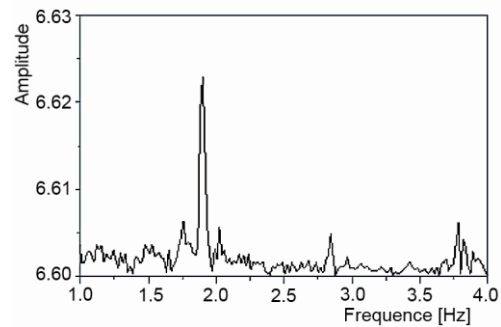


Figure 13. Velocity fluctuation specter

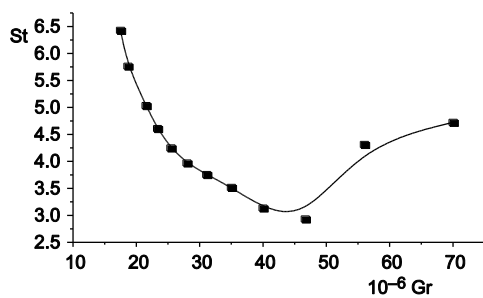


Figure 14. Variation of Strouhal number depending Grashof number

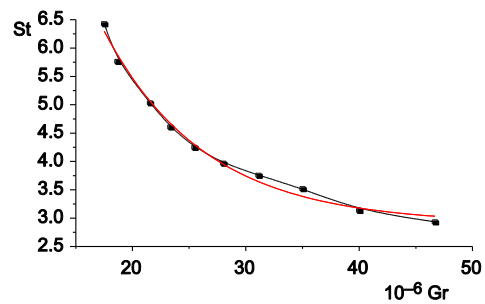


Figure 15. Correlation between Grashof and Strouhal numbers

Table 1

<i>A</i>	<i>U</i> [ms ⁻¹]	<i>F</i> [Hz]	<i>St</i>	10 ⁻⁶ <i>Gr</i>
1,00	0,08	1,92	3,43	93,37
1,33	0,08	1,89	4,73	70,03
1,67	0,11	1,95	4,31	56,02
2,00	0,18	1,78	2,93	46,69
2,33	0,20	1,81	3,14	40,02
2,67	0,21	1,87	3,52	35,01
3,00	0,23	1,92	3,76	31,12
3,33	0,24	1,93	3,97	28,01
3,67	0,26	1,97	4,25	25,46
4,00	0,26	2,02	4,61	23,34
4,33	0,27	2,06	5,03	21,55
5,00	0,27	2,06	5,76	18,67
5,33	0,28	2,21	6,43	17,51

The profile of change in the Strouhal number depending Grashof number (for $Gr < 50 \cdot 10^6$) and the correlation $St = 3 + 25 \exp(-Gr/9 \cdot 10^6)$, shows good agreement between the two.

Conclusions

In this study, it is shown that there is a good agreement between the experimental and numerical results. The first zone of the plume structure in the channel, has the same level of dimensionless Z^* corresponding to any channel height. It is also shown that the escape rate depends on the channel height and the Strouhal number remains constant for small channel heights.

The shape ratio A is greater than 2, and a good agreement between the variation of Strouhal number as a function of Grashof number, and a correlation of the form $St = 3 + 25 \exp(-Gr/9 \cdot 10^6)$ was found.

Nomenclature

<i>A</i> – shape ratio ($= L/D$)	T^* – dimensionless average temperature [$= (T - T_a)/(T_s - T_a)$]
<i>D</i> – channel width, [m]	<i>t</i> – time, [s]
<i>d</i> – source width, [m]	<i>U</i> – average velocity, [ms ⁻¹]
<i>F</i> – frequency at exhaust, [Hz]	<i>X</i> – horizontal co-ordinate, [m]
<i>Gr</i> – Grashof number { $= [g\beta(T_s - T_a)D^3]/Av^3$ }	X^* – dimensionless horizontal co-ordinate ($= X/L$)
<i>g</i> – acceleration of gravity, [ms ⁻²]	<i>Z</i> – vertical co-ordinate, [m]
<i>k</i> – thermal conductivity, [m ² s ⁻¹]	Z^* – dimensionless vertical co-ordinate ($= Z/L$)
<i>L</i> – channel height, [m]	<i>Greek symbols</i>
<i>p</i> – local pressure, [Pa]	β – thermal expansion coefficient, [°C ⁻¹]
<i>St</i> – Strouhal number ($= FL/U$)	ρ – density, [kgm ⁻³]
<i>T</i> – local average temperature, [°C]	ν – kinematic viscosity, [m ² s ⁻¹]
<i>T_a</i> – ambient temperature, [°C]	
<i>T_s</i> – source temperature, [°C]	

Reference

- [1] Tan, M., Opposite Sunspaces Passive Solar Air Heating System, *Solar Energy*, 60 (1997), 3-4, pp. 127-134
- [2] Bezian, J. J., Arnaud, G., Application of the Natural Convection in Inclined Cavities to Passive Solar Heating (in French), *Proceedings*, International Conference on Solar Architecture, Cannes, France, 1986, vol. 2, pp. 424-429
- [3] Mohamed, A. O., et al., Interaction of a Flow in Thermosiphon with a Thermal Plume in Axial Symmetry: Experimental Study (in French), *Rev. Gen. Therm.* 37 (1998), 5, pp. 385-396
- [4] Bouslimi, J., Dehmani, L., Experimental Investigation of the Thermal Field of a Turbulent Plume Guided Cylinder – Preliminary Results, *Exp. Ther. Fluid*, 29 (2005), 4, pp. 477-484
- [5] Zinoubi, J., et al., Influence of the Vertical Source-Cylinder Spacing on the Interaction of a Thermal Plume with a Thermosiphon Flow: an Experimental Study, *Experimental Thermal and Fluid Science*, 28 (2004), pp. 329-336
- [6] Ben Maad, R., Belghith, A., The Use of Grid-Generated Turbulence to Improve Heat Transfer in Passive Solar Systems, *Renewable Energy*, 2 (1992), 3, pp. 333-336
- [7] Gammoudi, A., et al., Experimental Study of a Thermal Plume Evolving in a Vertical Heated Channel: Influence of the Temperature of the Plume Source, *Int. Rev. Mech. Eng.*, 4 (2010), 3, pp. 288-296
- [8] Naffouti, T., et al., Experimental Characterization of a Free Thermal Plume and in Interaction with Its Material, Environment, *Applied Thermal Engineering*, 30 (2010), 13, pp. 1632-1643
- [9] Jouini, B., et al., Thermal Plume in a Vertical Channel: Effect of the Source-Channel Vertical Spacing, *Heat Transfer Research*, 42 (2011), 6, pp. 557-569
- [10] Ryder, N. L., et al., Consequence Modeling Using the Fire Dynamics Simulator, *J. Hazard. Mater.*, 115 (2004), 1-3, pp. 149-154
- [11] Ryder, N. L., et al., Near and Far Field Contamination Modeling in a Large Scale Enclosure: Fire Dynamics Simulator Comparisons with Measured Observations, *J. Hazard. Mater.*, 130 (2006), 1-2, pp. 182-186
- [12] Hu, L. H., et al., Modeling Fire-Induced Smoke Spread and Carbon Monoxide Transportation in a Long Channel: Fire Dynamics Simulator Comparisons with Measured Data, *J. Hazard. Mater.*, 140 (2007), 1-2, pp. 293-298
- [13] McGrattan, K., et al., *Fire Dynamics Simulator (Version 5.5) Technical Reference Guide*, NIST Special Publication 1018-5, 2010
- [14] McGrattan, K., et al., *Fire Dynamics Simulator (Version 5.5) User's Guide*, NIST Special Publication 1019-5, 2010
- [15] Smagorinsky, J., General Circulation Experiments with Primitive Equations, I – the Basic Experiment, *Monthly Weather Review*, 91 (1963), 3, pp. 99-105
- [16] Thomas, P. H., The Movement of Smoke in Horizontal Passages Against an Air Flow, Fire Research Note No. 723, Fire Research Station, Watford, UK, 1968